cells as a reaction to cytomegalovirus. The presence of an interference factor during the first 8 to 72 hours of in vitro CMV infections has been postulated by Glasgow (*5*) on the basis of experiments that demonstrated a lack of host cell susceptibility to invasion by a second virus. Another hypothesis is that CMV infection depresses DNA-dependent RNA synthesis, in the manner of closely related herpes viruses (*6*), and thereby deprives the toxoplasma of a vital protein supply. The latter possibility is not supported by preliminary experiments. Fibroblasts that were incubated with mitomycin C (50 μg/ml), actinomycin D (0.5 μg/ml), or puromycin (20 μg/ml) for ½ hour and washed prior to inoculation of parasites or infected in the presence of these antimetabolites sustained growth of the *Toxoplasma gondii* in a manner similar to control cultures.

The curious replication pattern of toxoplasma parasites in cells doubly infected with CMV may offer some clue as to their obligate nutritional requirements. In late CMV infection, there appears to be an overall increase in cytoplasmic volume, and fibroblasts assume many ultrastructural characteristics of macrophages. The Golgi zone hypertrophies, dense lysosomal bodies are numerous, and there is a measurable increase in the total content of acid phosphatase (*2*, *3*). The organelle structure of CMV-infected cells is also similar to macrophages in that mitochondria tend to accumulate around a cytocentrum (*7*). Toxoplasma parasites are confined to vacuoles within the cytoplasm of the host cell. Host cell mitochondria investing the parasite-filled vacuoles (Fig. 4) may be required by the parasites as a source of energy or they may serve to maintain a metabolic gradient within the parasite vacuole.

ALBERT H. GELDERMAN
PHILIP M. GRIMLEY
Pathologic Anatomy Branch, National Cancer Institute, Bethesda, Maryland 20014
MILFORD N. LUNDE
Laboratory of Parasitic Diseases, National Institute of Allergy and Infectious Diseases
ALAN S. RABSON
Pathologic Anatomy Branch, National Cancer Institute

References

1. W. M. Vietzke, A. H. Gelderman, P. M. Grimley, M. P. Valsamis, *Cancer*, in press.
2. M. H. McGavran and M. G. Smith, *Exp. Mol. Pathol.* **4**, 1 (1965).
3. B. H. Ruebner, H. Takuo, R. J. Slusser, D. N. Medearis, Jr., *Amer. J. Pathol.* **46**, 477 (1965).
4. M. C. Bowling, *Histopathology Laboratory Procedures* (U.S. Government Printing Office, Washington, D.C., 1967), p. 2.
5. L. A. Glasgow, *Bacteriol. Proc.*, abstr. No. V132 (1967), p. 156.
6. C. Sirtori and M. Bosisio-Bestetti, *Cancer Res.* **27**, 367 (1967); C. R. Goodheart, R. M. McAllister, J. E. Filbert, *Virology* **23**, 603 (1964); H. T. Wright and C. R. Goodheart, *ibid.*, p. 419.
7. Z. A. Cohn and E. Wiener, *J. Exp. Med.* **118**, 991 (1965).

7 February 1968

Dendritic Spikes and Their Inhibition in Alligator Purkinje Cells

Abstract. *Alligator Purkinje cells generate action potentials in the peripheral dendritic tree, after synaptic depolarization via superficial parallel fibers. These action potentials are inhibited at the dendrite level by preceding parallel-fiber volleys at close intervals. We conclude that this inhibition is produced by the activation of the inhibitory interneurons of the molecular layer, the stellate cells, which establish synaptic contacts with the dendrites of the Purkinje cells.*

Ramón y Cajal first hypothesized that neuronal dendrites receive and channel incoming information toward the axon, the neuron's output system (*1*).

In studying the anatomy of the Purkinje cell, one wonders how the distal region of the dendrites can act upon the soma and axon of this neuron. The two known mechanisms by which such distant dendrites can influence the activity of the cell are (i) by direct electrotonic spread from the distal dendrite to the soma, or (ii) by the initiation of action potentials or local responses which can be conducted either in an all-or-none manner or in a decremental fashion down to the axon.

The possibility that the large dendrites of Purkinje cells could generate action potentials has been suggested because they can be invaded antidromically after electrical stimulation of the underlying cerebellar white matter (*2*). We now present evidence that, in the alligator cerebellum, action potentials are initiated in peripheral dendrites after synaptic depolarization. Spike initiation, which can occur 50 to 150 μm from the dendritic terminals, is followed by a full-size action potential which is conducted towards the soma, possibly in a noncontinuous manner. Furthermore, this type of dendritic action potentials can be blocked at the dendritic level, most probably by inhibition mediated through the stellate interneurons of the molecular layer.

South American alligators (*Caiman sclerops*) ranging in size from 35 cm (200 g) to 67 cm (2 kg) were anesthetized with sodium thiopental (10 mg/km). The cerebellum was exposed by a craniotomy which left visible most of the medial lobe, the fissura secunda, and part of the posterior lobe (Fig. 1A). After removal of the dural membrane and the arachnoid tissue, the surface of the cerebellar cortex was accessible to electrical stimulation and recording. The molecular layer, the outermost layer of the cerebellar cortex, was activated by means of a bipolar metal electrode insulated to its tip (Fig. 1A). The field potentials generated in the cerebellum were recorded with micropipettes filled with 4*M* NaCl having an average d-c resistance of 2 to 3 megohms. The average response computation of the field potentials was carried out by means of a Fabri-Tek 1064 computer.

The alligator cerebellar cortex is uniquely suited for electrophysiological studies. It is in this animal, the only surviving member of the ruling reptiles (the Archeosaurus, from which stem the "dinosaurs" as well as the birds), where the first single-cell layer of Purkinje cells seems to appear in evolution (*3*).

The dendritic tree of alligator (Fig. 1B) grows out of the soma as a single stem, about 100 μm long, which then subdivides into two or three secondary branches which, in turn, bifurcate several times. Most of this tertiary bifurcation takes place in the superficial 250 μm of the molecular layer. In many cases, branches grow sideways or even downward towards the granular layer; but even in these instances, the length of the dendritic segment between the soma and the first bifurcation is about the same for the descending as for the ascending branches. The tertiary dendrites do not seem to decrease in diameter as much as those in other species, so that fairly thick dendrites can be found up to the surface of the cortex (Fig. 1B). The parallel fibers are

regularly distributed, running transversely and establishing synaptic junctions at all levels with the dendritic arbor, very much as in other animals (*4*). In contrast to the cerebellar cortex of the cat, the interneurons of the molecular layer in the alligator belong almost exclusively to the stellate type, there being no true basket cells in this animal (*4*). The stellate neurons receive axodendritic and axosomatic synaptic contacts from the parallel fibers (*5*), as reported for other forms (*6*), and, in turn, send axons at right angles to the parallel-fiber plane. The stellate terminals synapse, for the most part, on the main dendrites of the Purkinje cells (Fig. 2J), only a few terminals reaching the upper end of the Purkinje cell soma (*7*). Their location, in the molecular layer; their input, predominantly from parallel fibers; and the distribution of their axons, transverse to the axis of the folia, make these stellate interneurons very similar to the basket cells. However, their axon terminals do not form the tight "basket" arrangement around the lower soma and preaxon, which is the salient characteristic of all basket cells (*1, 8*).

Electrical stimulation of the surface of the cerebellum via a bipolar electrode (Fig. 1A) activates, as in cat (*9*) and frog (*10*), a bundle or beam of parallel fibers running transversely along the length of the folia through the Purkinje cell dendrites. This "beam" of activated parallel fibers is depicted as a dashed area on the surface (Fig. 1A). The dotted, rounded contour seen in the molecular layer over the Purkinje cell dendrite represents the bundle of parallel fibers normally activated by the local stimulation.

The parallel-fiber beam can be recorded with a microelectrode at the surface of the cerebellum (Fig. 1B). From this point, the microelectrode is pushed down into the cerebellar cortex, and recordings of the field potential can then be made at 50- or 100-μm steps as the microelectrode is withdrawn (Fig. 1, C and D). When the cerebellum is in good condition, the records obtained as the electrode reaches the surface again coincide with the control taken previous to the insertion of the microelectrode.

Following local stimulation there is an early, large, positive-negative transient (Fig. 1C) which is evoked by the compound action current generated by the approaching parallel-fiber volley (*9*, *10*). This parallel-fiber field is larg-

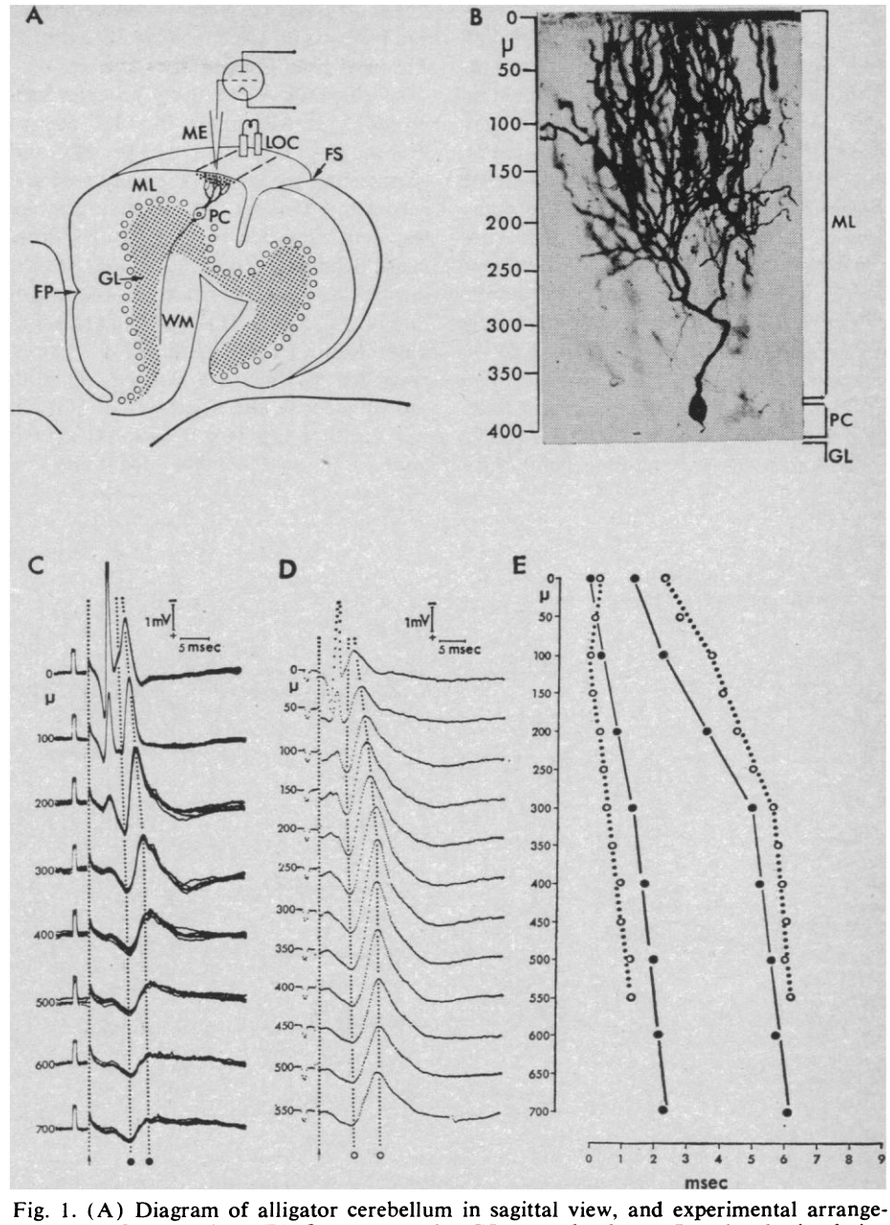

Fig. 1. (A) Diagram of alligator cerebellum in sagittal view, and experimental arrangement. *FP*, fissura prima; *FS*, fissura secunda; *GL*, granular layer; *Loc*, local stimulating electrode; *ME*, recording microelectrode; *ML*, molecular layer, *PC*, Purkinje cell layer; *WM*, white matter. (B) Typical alligator Purkinje cell stained by the rapid Golgi silver impregnation method. The scale to the left shows depth in microns from the surface of the cortex. This scale is to be related to the recording depths as illustrated in C, D and E. *ML*, molecular layer; *PC*, Purkinje cell layer; *GL*, granule cell layer. Note the considerable thickness of the dendritic terminal arborizations. (C and D) Field potentials recorded at different depths in the molecular layer after surface electrical stimulation of the cerebellar cortex. In (C) four traces are superimposed at each depth. The fields are recorded every 100 μm (see scale at the left of each record) as the electrode is withdrawn from a depth of 700 μm. The first dotted line marked by the arrow represents the stimulus artifact; the second dotted line, the foot of the dendritic compound action current; the third dotted line, the peak of the same component. D, as in C, from another experiment. Each trace is the computed average of 16 responses. The fields were recorded at 50 μm from each other. Time and voltage calibration as indicated. (E) Plot of the conduction velocity of the dendritic action currents illustrated in C and D. Abscissa time in milliseconds. Ordinate depth in microns. The two columns to the left represent the latency of the foot of the dendritic action currents for records C (closed circles) and D (open circles). Zero time is the shortest latency for the dendritic spikes at any depth; in C, this occurred at 50 μm, and in D, at 100 μm. The second column plots the latency of the peak of the dendritic action currents as measured from zero, as defined above. Note that in C the dendritic action currents seem to be initiated at 100 μm from the surface, and are then conducted upward and downward. The conduction velocity measured from the peak of the dendritic negativity shows two or three different rates of conduction, slower at the upper dendrites and faster at the lower level of the dendritic tree.

est at the surface and decreases in amplitude with depth such that at 200 μm it is, in fact, only a small potential. The parallel-fiber field is barely detectable at 150 μm (Fig. 1D). It is assumed that the beam is only 100 μm or so deep and that the small negativities observed at lower levels are produced by the compound action-current field which surrounds activated fiber bundles in volume conductors (*11*). The compound action current evoked by the parallel-fiber volley is followed at the surface by a longer-lasting negativity. This negativity has, in the alligator, a double component, a slow rising potential which follows immediately the parallel-fiber fields (Fig. 1, C and D, at 0 μm) and a faster negative-positive transient (second dotted line in Fig. 1, C and D).

The first slow negativity reverses to a positivity at 150 μm in Fig. 1C, and as superficially as 50 μm in Fig. 1D, and is present throughout the depth of the recording. The second negative-positive transient recorded at the surface, however, becomes larger at deeper levels, reaches its maximum value at 200 μm in Fig. 1C and 300 μm in Fig. 1D, and then subsides again with depth without reversing its polarity. As seen in both sets of records, the negativity at 150 μm has a rather fast rate of rise. At deeper levels, the onset of the negativity becomes progressively later, and its time course broadens. The peak of the negativity (third dotted line) is also delayed with depth. In Fig. 1C, the onset of the negativity occurs within the first 100 μm, and its latency increases at all levels below this depth (Fig. 1E). A similar result is obtained if the peak of the negativity is plotted. Very much the same results are obtained by plotting the onset and peak of the records shown in Fig. 1D. In this case, however, the negativity seems to be initiated 100 μm from the surface.

These records strongly indicate that after a local stimulation a current sink is generated which invades downwards with a conduction velocity of approximately 30 to 40 cm/sec for the fastest component (foot of the negative wave), of 10 cm/sec for the peak of the negativity in the first 300 μm, and of 40 cm/sec for the peak of the negativity from 300 μm downward. These values agree well with those published for motoneurons (*12*), motor cortex pyramidal cells (*13*), hypocampal pyramids (*14*), and cultured neurons (*15*).

In Fig. 2, A and B, are records showing interaction of fields at different depths. In Fig. 2B, a conditioning local stimulus (first dotted line) precedes a second local stimulus by 20 msec (second dotted line). The negativity seen in the control in Fig. 2A is completely blocked at all levels by the first local stimulus. This inhibition does not affect the parallel fiber negativity nor the synaptic current generated by the crossing-over synapses. Under these conditions, the synaptic current evoked by the second stimulus generates a field which is negative at the surface, has its zero isopotential level at 150 μm, and then reverses to a positive field at deeper levels (Fig. 2B).

Clearly the negative-positive transient, the only component of the field which is depressed by a preceding local stimulus, must be generated by action currents in the dendrites of Purkinje cells, and the increase in the latency of the negative field with depth corresponds to the conduction time of the action potentials in the dendrites as they are propagated towards the soma. The depression of the dendritic action current (DAC) reaches its maximum 12 msec after the conditioning shock and has completely recovered 50 msec later (Fig. 2, C and D). The time course of this inhibition correlates well with the duration of the inhibitory postsynaptic potential (40 to 50 msec) re-

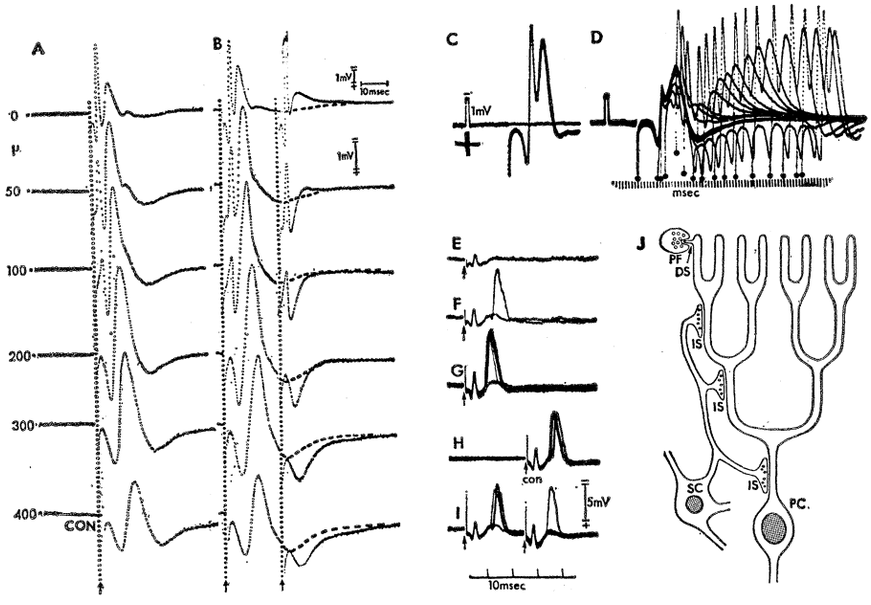

Fig. 2. (A and B) Field potentials recorded at different depths after paired stimulation of the surface of the cerebellum. Each record is the computed average of 16 responses. In A, control (CON) responses at different depths. The depths for A and B are as shown at the left of records A. (B) Complete block of second dendritic action currents by a preceding local stimulus at 20-msec interval, recorded at different depths. The surface (0 μm) the parallel-fiber volley (first positive-negative transient) is not changed from the control, but the dendritic negative-positive transient is lost, unmasking the typical negative wave generated by the excitatory synaptic current at the surface. This negative wave is reversed to a positivity at depths below 150 μm. The baseline for this field is marked by dashed lines. Arrows and dotted lines indicate the stimulus artifacts. Note that the amplitude calibration for the surface records is different from that for the rest of the traces. (C and D) Time course of the inhibition of the dendritic action currents following a preceding local stimulus. (C) Control field potential recorded near the surface of the cerebellar cortex. (D) The control local stimulus is presented at different intervals after a smaller fixed local stimulus. The stimuli are marked by filled circles. (E–I) Extracellular all-or-none dendritic action potentials recorded at 100 μm from the surface. (E) Weak local stimulus generating a small parallel-fiber field followed by the negative synapse wave. As the stimulus is slightly increased in magnitude (F), an all-or-none extracellular negative action potential of 7-msec duration is evoked. In (G), the stimulus is increased further, and the action potentials appear at a shorter latency; (H) is the control at a slightly stronger stimulus. In (I), a preceding submaximal local stimulus produced inhibition of the second action potential (*16*), with one exception. With stronger preceding stimulus, the inhibition is complete. (J) Diagram to illustrate the location of the excitatory and inhibitory synapses (*IS*). The parallel fibers (*PF*) are shown establishing excitatory synaptic contacts with the end terminal of the Purkinje cell dendrites on dendritic spines (*DS*). The inhibitory neuron, the stellate cell (*SC*), is shown establishing synaptic contacts on the main dendritic branches of the Purkinje cell.

corded in the soma of the alligator Purkinje cell after local stimulation (*7*).

On several occasions, all-or-nothing extracellular action potentials were recorded near the surface of the cortex (Fig. 2, E–I). These action potentials were in most instances negative and had a very prolonged time course with a slow, notched falling phase which suggests noncontinuous conduction. At the soma, single or repetitive positive-negative action potentials could be observed in the same experimental conditions. These have a short duration and are in every way similar to those recorded in cat or frog Purkinje cells (*9, 10*).

We conclude, therefore, that local stimulation of the surface of the alligator cerebellum evokes action potentials near the tip of the dendrites. These action potentials are conducted downward toward the soma. The conduction velocity is not uniform throughout the length of the dendrite, being rather slow at the surface and fastest at the level of the single dendritic stem and the axon. Similar potentials have been recorded in the pigeon cerebellum (*7*). In the pigeon, there is also the tendency for Purkinje cells to have only a single mainstem dendrite (*1, 3, 7*).

The blockage of the DAC is postulated to be produced by inhibitory action of stellate cells on the dendrites of Purkinje cells. Golgi and electron-microscopical studies of the alligator cerebellar cortex show that the axonal synapses of such stellate cells cover most of the dendrites from a depth of 150 μm to near the soma of the Purkinje cell (*5*). These interneurons, apparently forerunners of the basket cells of birds and mammals, can inhibit the dendritic spikes of Purkinje cells for a distance of up to 400 μm lateral to an excited beam of parallel fibers (*16*). This corresponds very well to the lateral extent of their axons.

From analyses of these and previous studies on the comparative aspects of cerebellar function, it seems probable that the cerebellum has undergone a gradual series of changes with evolution. In primitive cordates such as anura, which lack stellate and basket cells in the molecular layer, no long-lasting inhibition of Purkinje cells is demonstrable (*10*). In reptilia, aves and mammalia, on the other hand, this inhibition is present (*7*), but in the case of the reptiles, it seems to be restricted to the dendrites. Finally, the inhibitory synaptic system reaches its maximum action only in the more advanced forms, as the stellate cell terminals migrate giving rise to the "baskets" which cover the entire soma and axons of the Purkinje cells.

RODOLFO LLINÁS, CHARLES NICHOLSON
JOHN A. FREEMAN, DEAN E. HILLMAN
Institute for Biomedical Research, Chicago, Illinois 60610

References

1. S. Ramón y Cajal, *La Textura del Sistema Nervioso del Hombre y los Vertebrados* (Moya, Madrid, 1904).
2. J. C. Eccles, R. Llinás, K. Sasaki, *J. Physiol.* **182**, 316 (1966).
3. R. Nieuwenhuys, in *The Cerebellum, Progress in Brain Research*, C. A. Fox and R. Snider, Eds. (Elsevier, Amsterdam, 1967), pp. 1–93.
4. O. Larsell, *J. Comp. Neurol.* **54**, 357 (1932).
5. D. E. Hillman, unpublished information.
6. C. A. Fox, K. A. Siegesmund, C. R. Dutta, in *Morphological and Biological Correlates of Neural Activity*, M. M. Cohen and R. Snider, Eds. (Harper and Row, New York, 1964), pp. 112–141; J. Hámori and J. Szentágothai, *Acta Biol. Hung.* **15**, 95 (1965).
7. R. Llinás, D. E. Hillman, W. Precht, *Proc. Dallas Neurolog. Symp.* (1968); in press.
8. S. Ramón y Cajal, *Rev. Trim. Histol. Norm. Patol.* **1**, 305 (1888).
9. P. Andersen, J. C. Eccles, P. E. Voorhoeve, *J. Neurophysiol.* **27**, 1138 (1964); J. C. Eccles, R. Llinás, K. Sasaki, *Exp. Brain Res.* **1**, 17 (1966).
10. R. Llinás and J. Bloedel, *Science* **155**, 601 (1967).
11. R. Lorente de Nó, *Stud. Rockefeller Inst. Med. Res.* **132** (1947).
12. R. Lorente de Nó, *J. Cell. Comp. Physiol.* **29**, 207 (1947); P. Fatt, *J. Neurophysiol.* **20**, 27 (1957).
13. C. G. Phillips, *Quart. J. Exp. Physiol.* **44**, 1 (1959); in *The Nature of Sleep*, G. E. W. Wolstenholme and M. O'Connor, Eds. (Churchill, London, 1961), pp. 4–24.
14. B. G. Cragg and L. H. Hamlyn, *J. Physiol.* **129**, 608 (1955); P. Andersen, *Acta Physiol. Scand.* **48**, 178 (1960).
15. W. Hild and I. Tasaki, *J. Neurophysiol.* **25**, 277 (1962).
16. R. Llinás, W. Precht, S. Kitai, unpublished information.

21 March 1968

Neonatal Castration: Influence on Neural Organization of Sexual Reflexes in Male Rats

Abstract. *Most male rats castrated 4 days after birth and given exogenous testosterone in adulthood were sexually motivated but incapable of completing the mating sequence with an ejaculatory response. When tested for sexual reflexes after spinal transection, these animals displayed impairment of genital responses. Similarly treated 12-day castrates exhibited a complete mating sequence and had normal sexual reflexes. Thus neonatal testicular androgen appears to have an organizational influence at the spinal level on neural tissue mediating sexual reflexes.*

It is believed that gonadal androgen has two roles in influencing sexual behavior of male mammals (*1*): one concerns the influence of androgen in the prenatal or early postnatal organization of neural tissue that mediates sexual behavior; the second concerns the postpubertal activation of previously organized neural tissue, resulting in the onset of mature patterns of sexual behavior. In support of this concept, several experiments (*1*, *2*) have demonstrated that most male rats, castrated on or before the 4th or 5th day after birth and given exogenous testosterone in adulthood, show a high degree of sexual motivation when tested with receptive females (indicated by the frequent occurrence of mounts and copulatory intromissions), but apparently cannot complete the mating sequence, as is shown by the absence of an ejaculatory pattern. Most male rats castrated after 10 days of age exhibit the complete mating pattern, characterized by several copulatory intromissions (normally five to 15) followed by an ejaculation. I was concerned with localization of the part of the central nervous system that is apparently organized by the neonatal androgen environment and irreversibly altered by neonatal castration.

The subjects were 17 Long-Evans male rats castrated 4 days after birth and 12 male rats castrated 12 days after birth. At 30 days of age the subjects were weaned and housed singly. Starting at 85 to 90 days of age, the subjects were daily injected subcutaneously with about 60 μg of testosterone propionate in oil per 100 g of body weight; injections were continued until the end of the experiment. In neonatal castrates given testosterone in adulthood, a frenulum is retained extending between the ventral surface of the penis and the preputial sheath. Therefore, in order to allow subjects to penetrate the females completely during intromission, the penile frenula of both 4-day and 12-day castrates were cut (ether anesthesia) 10 to 24 days after initiation of the hormone injections.